molecular pharmaceutics

ARTICLE

pubs.acs.org/molecularpharmaceutics

Augmented Anticancer Efficacy of Doxorubicin-Loaded Polymeric Nanoparticles after Oral Administration in a Breast Cancer Induced Animal Model

Amit K. Jain, Nitin K. Swarnakar, Manasmita Das, Chandraiah Godugu, Raman Preet Singh, Poduri Rama Rao,† and Sanyog Jain*

Centre for Pharmaceutical Nanotechnology, Department of Pharmaceutics, National Institute of Pharmaceutical Education and Research (NIPER), Sector 67, SAS Nagar (Mohali), Punjab 160062, India

ABSTRACT:

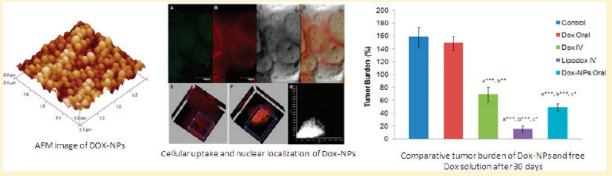

The present investigation reports an extensive evaluation of in vitro and in vivo anticancer efficacy of orally administered doxorubicin-loaded poly(lactic-co-glycolic acid) (PLGA) nanoparticles (Dox-NPs) in a breast cancer induced animal model. Spherically shaped Dox-NPs were prepared with an entrapment efficiency and particle size of 55.40 ± 2.30% and 160.20 ± 0.99 nm, respectively, and freeze-dried with 5% trehalose using stepwise freeze-drying. Cytotoxicity, as investigated on C127I cell line, revealed insignificant differences between the IC_{50} of free Dox and Dox-NPs treated cells in the first 24 h, while higher cytotoxicity was demonstrated by Dox-NPs, following 72 h of incubation. Confocal laser scanning microscopy (CLSM) imaging corroborated that nanoparticles were efficiently localized into the nuclear region of C127I cells. The cellular uptake profile of Dox-NPs revealed both time and concentration dependent increases in the Caco-2 cell uptake as compared to the free Dox solution. Further, Dox-NPs significantly suppressed the growth of breast tumor in female Sprague−Dawley (SD) rats upon oral administration. Finally, orally administered Dox-NPs showed a marked reduction in cardiotoxicity when compared with intravenously injected free Dox as also evident by the increased level of malondialdehyde (MDA), lactate dehydrogenase (LDH), and creatine phosphokinase (CK-MB) and reduced levels of glutathione (GSH) and superoxide dismutase (SOD). The reduced cardiotoxicity of orally administered Dox-NPs was also confirmed by the major histopathological changes in the heart tissue after the treatments of intravenously injected free Dox and orally delivered Dox-NPs.

KEYWORDS: doxorubicin, PLGA nanoparticles, nuclear localization, oral delivery

1. INTRODUCTION

Doxorubicin (Dox) is a chemotherapeutic anthracycline antibiotic, widely used for the treatment of wide range of cancers including hematological malignancies, carcinomas, and sarcomas. It is also used in the treatment of leukemia, Hodgkin's lymphoma, cancers of the bladder, breast, stomach, lung, ovaries, thyroid, and soft tissue, sarcoma, and multiple myeloma.[1] Dox is known to interact with the DNA by intercalation, which in turn, inhibits the biosynthesis enzyme topoisomerase II while unwinding DNA transcription.[2]

Dox is commonly administered intravenously in the form of commercially available injections Adriamycin and Rubex for maintaining the therapeutics levels in blood.[3] In addition, two PEGylated liposomal formulations of Dox, that is, Doxil[4] and Caelyx,[5] are also available. However, intravenously administered Dox causes initial rapid increase and successive fall in blood levels below the therapeutic levels of drug, which necessitates frequent administration of Dox, thereby leading to serious side effects. Apart from these, acute cardiotoxicity is another major problem associated with the Dox therapy. It causes the free radical generation[6] by the two pathways leading to the generation of a Dox semiquinone free radical and anthracycline free radicals, respectively.[7,8] Radical generation via either pathways deplete the cellular component of cells and causes the cardiomayopathy.[9] Doxorubicinol, the major metabolite of Dox, is also reported to cause the cardiotoxicity.[10] A variety of novel carriers have been reported, where an attempt has been made to reduce the cardiotoxicity of Dox after intravenous administration, like novel pectin-adriamycin conjugate,[11] *N*-(2-hydroxypropyl) methacrylamide conjugates of Dox,[12] Dox-loaded poly(butyl cyanoacrylate) nanoparticles,[13] Dox-loaded polymersomes,[14] polyisohexylcyanoacrylate nanoparticles,[15] dextran-Dox/chitosan nanoparticles,[16,17] hyaluronic acid-anchored

Received: January 11, 2011
Accepted: May 10, 2011
Revised: April 29, 2011
Published: May 10, 2011

poly(lactic-co-glycolic acid) (HA-PEG-PLGA) nanoparticles,[18] core−corona nanoparticles of hyaluronic acid−polyethyleneglycol−polycaprolactone (HA-PEG-PCL) copolymer,[19] and many more.

The peroral route of drug administration is considered as the most natural, convenient, and safest route of drug administration involving higher patient compliance, less complications, and cost-effectiveness as compared to parental drug delivery.[20] However, Dox shows very poor oral bioavailability (<5%) due to its extensive first pass extraction and overexpression of P-glycoprotein (P-gp) efflux in the intestinal gut lumen.[21] Although the suppression of P-gp efflux system by some P-gp inhibitors could enhance the oral bioavailability of Dox, the technique is severely fraught with certain immunological and medical complications.

In recent years, the exploitation of nanocarriers for oral application has experienced phenomenal strides. Biodegradable nanoparticles constitute one of the most widely employed carriers for the delivery of anticancer drug molecule. Among all of them, poly(lactic-co-glycolic acid) (PLGA) is an FDA (Food and Drug Administration) approved biocompatible, biodegradable, and safely administered polymer and widely employed for loading and encapsulation of variety of anticancer drugs.[21−23] Like other nanoparticulate carriers, PLGA nanoparticles are also taken up by the specialized M cells overlaying the Peyer's patches in the small intestine and directly absorbed into lymphatics.[24−26] By this way, first pass metabolism in the liver and P-gp efflux pump present in the intestinal lumen can be effectively bypassed.[27−29] Recently, we have shown that formulation of tamoxifen within PLGA nanoparticles enhances the oral bioavailability of tamoxifen by 3.84 and 11.19 times, when compared to its salt form and free base, respectively.[29]

Dox-loaded PLGA nanoparticles for oral bioavailability enhancement have been earlier developed by Kalaria et al. at the Centre for Pharmaceutical Nanotechnology, Department of Pharmaceutics, National Institute of Pharmaceutical Education and Research (NIPER).[21] They reported 363% enhancement in the oral bioavailability of Dox using PLGA nanoparticles. However, to realize the actual potential of Dox-loaded nanoparticles (Dox-NPs) in the chemotherapeutic regimen, the prepared formulation requires a thorough evaluation in terms of various pharmacodynamic aspects. The present work thus stemmed in from the necessity to investigate the in vivo antitumor efficacy of PLGA-Dox NPs after oral administration in the DMBA-induced breast tumor model and develop a meaningful in vitro−in vivo correlation with regards to their intestinal epithelial permeability and anticancer efficacy. In course of extensive in vitro studies, we have nicely demonstrated the cytotoxicity and nuclear localization of Dox-NPs in mouse breast cancer cell line C127I.[30] We further sought to demonstrate the intestinal epithelial permeability of Dox-NPs by conducting cellular uptake studies in the Caco-2 cell model. A P-gp inhibition experiment by cyclosporine A (Cys-A) correlates the uptake of Dox NPs by the specialized M-cells in the intestine, while free Dox is minimally transported by the enterocytes present in the GIT tract. Finally, in course of an extensive toxicological evaluation, we demonstrated that orally administered Dox-NPs shows a marked reduction in cardiotoxicity as compared to intravenously administered free Dox.

2. MATERIALS AND METHODS

2.1. Materials. Doxorubicin hydrochloride (99.9%) was a kind gift from Sun Pharma Advanced Research Centre (SPARC), India, and Cyclosporin A (Cys A) was obtained from Panacea Biotech (Mumbai, India) as a gift sample. PLGA 50/50 (inherent viscosity 0.41 dL/g in chloroform at 25 °C) was used from Boehringer Ingelheim (Ingelheim, Germany). Poly(vinyl alcohol) (PVA) (MW = 30000−70000), 7,12-dimethylbenz[α]-anthracene (DMBA), trypsin-ethylenediaminetetraacetic acid (EDTA), MTT (3-(4,5-dimethyl-2-thiazolyl)-2,5-diphenyl-2*H*-tetrazolium bromide), coumarin-6, Triton X-100, and acridine orange (AO) were obtained from Sigma, USA. Dulbecco's modified Eagle's medium (DMEM), fetal bovine serum (FBS), antibiotics (antibiotic−antimycotic solution), and Hanks's balanced salt solution (HBSS) were purchased from PAA, Austria. Tissue culture plates and eight-well culture slides were procured from Tarsons and BD Falcon, respectively. Ethyl acetate (LR grade), acetonitrile (high-performance liquid chromatography (HPLC) grade), and glacial acetic acid (HPLC grade) were purchased from Ranchem Fine Chemicals, India. Lipodox was purchased from the local supplier. Ultra pure water (SG water purification system, Barsbuttel, Germany) was used through the experiments. All other reagents used were of analytical grade and purchased from local suppliers unless mentioned.

2.2. Preparation of Freeze-Dried Dox-Loaded Nanoparticles (Dox-NPs). Dox-NPs were prepared by the double emulsion diffusion evaporation method as reported earlier in literature with slight modifications.[21] Briefly, 50 mg of PLGA was dissolved in 2.5 mL of ethyl acetate. An aqueous solution of Dox (5 mg in 500 μL) was dispersed in the organic phase with constant stirring. The resulting primary emulsion was then sonicated for 30 s with a probe sonicator (Misonix, USA) at 60 amplitude. The primary emulsion was then emulsified in 2% (w/v) PVA solution under magnetic stirring to form a w/o/w emulsion. The final double emulsion was then sonicated for 60 s and diluted in a large volume (20 mL) of water to get the Dox-NPs. The NP suspension was then centrifuged and washed repeatedly to remove the excess surfactant and freeze-dried (Vir Tis, Wizard 2.0, New York, USA, freeze-dryer) following an optimized freeze-dried cycle. The condenser temperature was −60 °C, and the pressure applied in each step was 200 Torr. The washed NP suspension (2 mL) was filled in 5 mL glass vials and subjected to freeze-drying using 5% (w/v) of trehalose. After freeze dying the Dox-NPs were characterized for the appearance of the cake, reconstitution time, size after freeze-drying, and entrapment efficiency.

2.3. Characterization of Nanoparticles. *2.3.1. Particle Size and Zeta Potential Measurement.* Dox-NPs were evaluated for their mean particle size, polydispersity index (PDI), and zeta potential by using Zeta Sizer (Nano ZS, Malvern Instruments, UK). All of the values were taken by the average of six measurements. The zeta potential was estimated on the basis of electrophoretic mobility under an electric field, as an average of 30 measurements.

2.3.2. Morphology of Dox-NPs. Dox-NPs were characterized for their surface morphology by atomic force microscopy (AFM) (Veeco Bioscope II, USA). Briefly, Dox-NPs suspension was placed on the silicon wafer by a micro pipet and air-dried. The microscope is vibration damped, and measurements were made using commercial pyramidal Si_3N_4 tips (Veeco's, CA, USA). The cantilever used for scanning was having length 325 μm and width 26 μm (tip diameter 117 nm) with a nominal force constant 0.1 N/m. Images were obtained by displaying the amplitude signal of the cantilever in the trace direction and the height signal in the retrace direction, both signals being simultaneously recorded.

2.3.3. Entrapment Efficiency. The percentage of drug encapsulated in PLGA NPs was determined by using a validated HPLC method reported in literature with slight modifications.[21] Briefly, the Dox-NPs suspension was centrifuged at 25 000 rpm, and the obtained pellet was dissolved in acetonitrile and estimated for drug content using a Shimadzu HPLC system consisting of a florescence detector and dVR Agilent Technologies Lichrospher 100 RP-18e end-capped 5 μm column (Germany). Acetonitrile, 10 mM acetate buffer (pH 3), and methanol (40:55:5 v/v) were used as the mobile phase with a flow rate of 1.0 mL/min. The injection volume was 10 μL, and the retention time of Dox was found to be 4.7 min. The Dox was analyzed by fluorimetric measurements at 470 nm (excitation) and 550 nm (emission).

2.4. Cell Culture Experiments. *2.4.1. Cells.* The C127I mouse breast cancer cell line was obtained from National Centre for Cell Sciences, Pune, India. The cells were maintained in a complete medium containing DMEM (PAA, Austria), 10% FBS (PAA, Austria), and antibiotics (antibiotic−antimycotic solution; PAA, Austria).

2.4.2. In Vitro Anticancer Activity. Breast cancer cells (1×10^5cells/well) were seeded in 96 well tissue culture plates. The plates were incubated overnight to allow the attachment of cells. The cell monolayers were then incubated with free Dox or Dox-NPs for 24 or 72 h. In recovery experiments, cells were incubated with free Dox or Dox-NPs for 24 h. The drug/NP containing medium was replaced with a drug-free medium and further incubated for 48 h. The cell viability was determined by MTT assay after drug/NPs treatment.

2.4.3. MTT Assay. After treatment, the cells were incubated with MTT (0.5 mg/mL; 0.2 mL) for 3 h, and the formazan concentration was determined spectrophotometrically at 550 nm (μQuant, Bio-Tek Instruments).

2.4.4. Cell Uptake Studies. C127I monolayers were incubated with 100 μg/mL Dox-NPs for 3 h and fixed with 3% paraformaldehyde (Merck, India). The nuclei were stained with 10 μg/mL AO (Sigma, USA). The cellular uptake and intracellular localization was observed by confocal microscopy (Olympus FV1000).

2.5. Uptake Studies of Dox-NPs by Caco-2 Cells. The cellular uptake of Dox-NPs and Free Dox was established by the Caco-2 cell culture experimentation.[31−33] Cell uptake studies was carried out with the Caco-2 cells (American Type Culture Collection), grown in 25 cm^2 tissue culture flasks at a density of 50 000 cells/well of the plate and maintained in 5% CO_2 atmosphere at 37 C. The cell medium was supplemented with a culture medium, DMEM, supplemented with 10% FBS, 100 U/mL penicillin, and 100 mg/mL streptomycin (PAA, Austria). The media was changed at every 2 day interval. After the attainment of 90% confluence in the cell culture medium, the collection of cell was done in 0.25% trypsin-EDTA solution (Sigma) further cultured in a 96 well black plate (Costars, Corning Incorporated) at a density of 2×10^4 cells/well for the further cellular uptake studies. Further the cells were incubated with the 100 mL of HBSS (PAA, Austria) for 1 h. After removing the HBSS solution from the cell culture medium, 500 μL of Dox solution or Dox solution mixed with Cys A or Dox-NPs (equivalent to 15 μM of Dox) was added to each plate for the cellular uptake studies. All of the dilutions were carried out in the HBSS, and blank Hank's solution was employed as the negative control. The supernatant was removed at the different time intervals (5−60 min), and cells were washed with ice-cold PBS (pH 7.6) and lysed with PBS containing 1% Triton-X. Dox concentrations in the cell lysates were measured with a microplate fluorometer (excitation wavelength λ_{ex} = 478 nm; emission wavelength λ_{em} = 594 nm). In another experiment, a different concentration (5−100 μM) of Dox solution or Dox-NPs was added into each well for the cellular uptake studies, and cells were incubated for 20 min. A Bradford colorimetric assay was employed for the protein determination in the cell lysate.[34]

2.6. In Vivo Antitumor Efficacy. *2.6.1. Tumor Induction.* Female Sprague−Dawley (SD) rats of 220−230 g and 7−8 weeks old were supplied by the Central Animal Facility (CAF), NIPER, India. All animal study protocols were duly approved by the Institutional Animal Ethics Committee (IAEC) of National Institute of Pharmaceutical Education and Research (NIPER), India. The animals were acclimatized at a temperature of 25 ± 2 °C and relative humidity of 50−60% under natural light/dark conditions for one week before experiments. 7,12-Dimethylbenz[α]anthracene (DMBA) in soya bean oil was administered orally to rats at a 45 mg/kg dose at weekly intervals for three consecutive weeks. A measurable tumor size was observed in the animals, and tumor bearing animals were separated.

2.6.2. Treatment. Drug treatment was given after 10 weeks of the last dose of DMBA, and animals were divided randomly into five different treatment groups. The control group (Group I) received an oral administration of PBS (pH 7.4). The II group of animals received an oral administration of free Dox. III and IV groups were treated with free Dox and Lipodox respectively administered intravenously. Finally, Dox-NPs were orally administered to group V. A dose equivalent to 5 mg/kg body weight, of Dox was kept in all the treatment of Dox formulations. The tumor width (w) and length (l) were recorded with an electronic digital caliper and tumor size was calculated using the formula ($l \times w^2/2$). The tumor size was measured up to 30 days (during the treatment period).

2.6.3. Kaplan−Meier Survival Analysis. The survival of the treated animals was investigated in a separate group of animals up to 60 days, and the data were analyzed by the Kaplan−Meier survival plot.

2.7. Cardiotoxicity Evaluation. The cardiotoxicity of different formulations was determined in breast tumor induced SD female rats. The animals were randomly divided in five groups. Group I was kept as the control without any treatment, group II received oral administration of free Dox at a single dose (10 mg/kg), group III and IV received free Dox and Lipodox intravenously (10 mg/kg), and Dox-NPs was orally administered to group V (10 mg/kg). The body weight of the animals was taken after every 48 h during the study period. After 21 days of administration of different formulations, blood samples were drawn from the retro orbital plexus under light ether anesthesia into heparinized capillary tubes. Plasma was separated by centrifugation at 5000 rpm for 5 min and stored at −20 °C until analysis. Dry weights of representative heart tissues from each group were taken for the calculation of heart-body weight index. Enzyme activities such as CK-MB (creatine phosphokinase) and LDH (lactate dehydrogenase) levels were analyzed in plasma while malondialdehyde (MDA), glutathione (GSH), and superoxide dismutase (SOD) were determined in heart homogenate by the commercially available kits based on the method provided by the manufacturer instructions supplied with the commercial kits. Representative heart tissues from each group were excised and fixed in 10% (v/v) formalin saline and processed for routine histopathological procedures. Paraffin embedded specimen were

Table 1. Particle Size, PDI, and Entrapment Efficiency of Dox-NPs[a]

formulation	theoretical drug loading (%)	particle size (nm)	zeta potential (mV)	PDI	entrapment efficiency (% w/w)
Dox-NPs	10%	160.20 ± 0.99	2.54 ± 0.56	0.034 ± 0.002	55.40 ± 2.30

[a] Values are expressed as mean ± SD (n = 6).

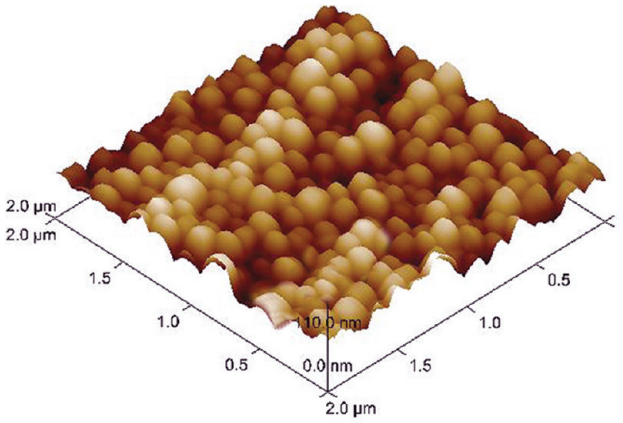

Figure 1. AFM image of Dox-NPs.

cut into 5 μm sections and stained with hematoxylin and eosin (H&E) for histopathological evaluations.

2.8. Statistical Analysis. All of the results were expressed as the mean ± standard deviation (SD). Statistical analysis was performed with Sigma Stat (Version 2.03) using one-way analysis of variance (ANOVA) followed by the Tukey−Kramer multiple comparison test. $P < 0.05$ was considered as statistically significant.

3. RESULTS

3.1. Preparation and Characterization of Nanoparticles. Table 1 shows the particle size, PDI, zeta potential, and entrapment efficiency of the prepared nanoparticles. They had good encapsulation efficiency (55.40 ± 2.30% at 10% w/w of polymer weight of initial theoretical drug loading), small particle size (160.20 ± 0.99 nm), and a narrow size distribution (0.034 ± 0.002). Dox-NPs showed the zeta potential 2.54 ± 0.56 mV.[21,29,35] An AFM image of nanoparticles shows distinct spherical particles with smooth surface (Figure 1). A good correlation was obtained in the size measured by zeta sizer and AFM analysis of Dox-NPs.

3.2. Freeze-Drying of Dox-NPs. Dox-NPs were freeze-dried following the stepwise freeze dying cycle reported by the Jain and co-workers.[35] A 5% (w/v) trehalose was employed as a cryoprotectant which was added to the nanoparticulate dispersion. After freeze-drying, the obtained cake was redispersed in 2 mL of distilled water, and the particle size along with PDI after freeze-drying was analyzed using a zetasizer. Redispersed Dox-NPs were evaluated for different properties like physical appearance, reconstitution nature, and size ratio (before and after freeze-drying) (Table 2). It is evident from Table 2, that 5% trehalose after lyophilization produced the intact fluffy cake that could be easily redispersed by mere shaking. The ratio of particle size before and after freeze-drying was determined and found to be almost unity. On the other hand significant ($p < 0.05$) increases in particle size with unusual PDI (>0.4) of NPs were observed when Dox-NPs were freeze-dried without trehalose. Moreover the NPs freeze-dried in absence of trehalose required shear vortexing for 2 min for reconstitution; even then cake was not completely redispersed, and some agglomerate of the particles was observed. No significant difference in percentage entrapment efficiency ($p > 0.05$) was observed before and after freeze-drying in all cases.

3.3. Cell Culture Experiments. *3.3.1. Cell Cytotoxicity Assay (MTT Assay).* The in vitro anticancer activity of free Dox and Dox-NPs was similar after 24 and 72 h of incubation (Table 3). The difference in IC_{50} values of free Dox and Dox-NPs was insignificant ($p > 0.05$) after both 24 and 72 h of incubation. However, in recovery experiments, the recovery of cells after an initial exposure to NPs was significantly ($p < 0.01$) lower as compared to the free drug.

3.3.2. Cell Uptake Studies. The cellular uptake of Dox-NPs was rapid, and NPs were detectable intracellularily after 3 h of incubation. Figure 2A−D shows the cellular uptake of Dox-NPs. Figure 2 parts E and F are three-dimentional reconstructions showing nuclear delivery of NPs. Quantitative colocalization analysis showed that more than 50% of NPs resided in the cell nucleus (Figure 2G). The localization of the Dox-NPs within the nucleus was also confirmed by the Pearson's coefficient (r) which was found to be 0.78. Similarly, box (Figure 3) and line (Figure 4) analysis also showed colocalization of Dox and AO fluorescence.

3.3. Uptake Studies of Dox-NPs by Caco-2 Cells. The time course of Dox uptake from Dox solution and Dox-NPs by the Caco-2 cells has been given in Figure 5. The Dox-NPs showed the significantly higher drug uptake at all of the time points as compared to the free drug solution. Moreover, the drug uptake from the Dox-NPs showed the plateau at the later time points. In the presence of Cys A (10 μg/mL) the Dox uptake was somewhat increased, but it was significantly ($p < 0.001$) lower than Dox uptake in case of Dox-NPs.

Similarly, when the concentration of Dox in the culture medium was increased, uptake by the Caco-2 cells was also increased as revealed in Figure 6. Dox-NPs showed significantly ($P < 0.001$) enhanced Caco-2 cellular uptake at all the concentration ranging from 10 to 90 μmol/L as compared to the free Dox solution.

3.4. In Vivo Antitumor Efficacy. Figure 7 shows the comparative antitumor efficacy of Dox-NPs after single oral administration, free Dox (administered by single IV and oral route), and marketed Dox formulation (Lipodox) administered intravenously. In the initial period of study, intravenously administered free Dox revealed significantly higher tumor growth suppression than orally administered Dox-NPs. However, in the later course of study, tumor growth in animals which received free Dox intravenously became static, whereas orally administered Dox-NPs incessantly decreased the tumor growth. After 30 days, tumor size was reduced up to 49.06% and 69.28% with orally administered Dox-NPs and intravenously administered free Dox respectively. On the contrary, the untreated groups showed an increase in tumor size up to 158.66% as compared to tumor

Table 2. Particle Size and PDI of Dox-NPs before and after Freeze Drying[a]

formulation	before freeze-drying			after freeze-drying					
	particle size (nm)	PDI	entrapment efficiency (% w/w)	particle size (nm)	PDI	entrapment efficiency (% w/w)	ratio (S_f/S_i)	physical appearance	reconstitution score
NPs with trehalose	161.20 ± 1.54	0.067 ± 0.032	54.40 ± 1.56	170.20 ± 1.24	0.104 ± 0.045	54.40 ± 1.37	1.055	intact fluffy cake	[b]
NPs without trehalose	160.67 ± 0.54	0.084 ± 0.056	54.40 ± 1.56	205.20 ± 3.54[c]	0.484 ± 0.256	55.70 ± 1.67	1.277	collapsed cake	[d]

[a] Values are mean ± SD ($n = 6$); S_f/S_i is the ratio of particle size after freeze drying to particle size before freeze drying. [b] Reconstitution in 1 mL of water and cake is easily redispersed within 20 s by mere shaking. [c] The size was measured after separation of large aggregates by centrifugation. [d] Reconstitution requires high shear vortexing for 2 min, but the cake was not completely redispersed, so some agglomeration was observed.

Table 3. IC_{50} Values (μg/mL) of Free Dox and Dox-NPs

formulation	24 h	72 h	recovery
free Dox	5.5	3.1	3.9
Dox-NPs	5.3	2.9	3.1[a]

[a] $P < 0.01$ wt free Dox.

volume before the start of treatment that was considered to be 100%. A single IV administration of marketed Dox formulation (Lipodox) decreased the tumor growth up to 84.94% which was significantly ($p < 0.05$) higher than tumor growth suppressed by orally administered Dox-NPs. Moreover, the animal group, which received free Dox orally showed a continuous increase in tumor size up to 149.18%. Figure 8 represents the tumor burden on rats 30 days after the start of treatment. Significant reduction ($p < 0.01$) in the tumor burden was observed after 30 days in animal group which received oral Dox-NPs, as compared to animal group which received the free Dox intravenously. In a parallel study, the survival of animals was monitored in other groups of animals which received a similar treatment for 60 days. The Kaplan−Meier survival curve (Figure 9) was plotted for survival analysis of different Dox formulations. The Dox-NPs enhanced the survival of 83.33% of animals up to 58th day. On the other hand, animal deaths occurred on 21st, 36th, 43rd, 55th, and 57th in the case of animal group treated with free Dox intravenously and on 13th, 32nd, 38th, 54th, 56th, and 59th of animal groups treated with oral free Dox. Intravenously Lipodox treated group of animals also did not show any sign of mortality until the end of the study.

3.6. Cardiotoxicity Evaluation. Orally administered Dox-NPs showed marked reduction in the cardiotoxicity as compared to intravenously injected free Dox, as evidenced from the different cardiotoxicity marker levels. It is evident from the Figure 10A−C that after 1 month MDA and LDH levels in heart tissue and CK-MB level in the plasma were significantly ($p < 0.001$) increased in the animal group which received free Dox intravenously. MDA, LDH, and CK-MB levels were also increased in the animals group treated with the Lipodox formulation as compared to the control group of animals ($p < 0.05$ for both MDA and LDH levels; $p < 0.01$ for CK-MB level). An insignificant ($p > 0.05$) difference was observed in the MDA and LDH levels after oral administration of free Dox. At the same time GSH and SOD levels in the heart homogenate decreased in the same group of animals (Figure 10D,E). A significant recovery ($p < 0.05$) to the normal level was observed in the cardiotoxicity marker levels in the animal group which received Dox-NPs orally.

Figure 11 shows the weight of heart excised from the representative animal after 21 days. As it is clear from the figure, dry heart weight was reduced significantly after the treatment of free Dox intravenously. On the contrary, the weight of heart excised from other treated groups was comparable as to the control group ($p > 0.05$). Conventional histopathological examinations of the representative heart tissue from each treatment group were carried out to determine the possibility of Dox induced cardiotoxicity in rats. As evident from the control group heart sections, normal striated cells can be seen with one or two nuclei centrally in the cells. The animal group treated with intravenously administered free Dox showed a marked degeneration of cardiac muscles characterized by the disorganization of the cardiac muscles, edema of cells, and vacuolization of cells, as evident from the histopathology section. Moreover, some mild damage to heart muscle fibers in the form of focal fragmentation and scanty number of macrophages was observed in case of animals treated with intravenously administered free Dox. Notably, no significant changes were found in the cardiac muscles treated with the marketed formulation, that is, Lipodox. On the contrary, animal groups treated with the oral Dox-NPs showed the minimal degeneration of cardiac muscles (Figure 12).

4. DISCUSSION

PLGA has been employed as a versatile polymer for the oral delivery of different anticancer drugs including the Dox.[21] Orally administered PLGA nanoparticles have been very well proven to absorb predominantly via the M cells in the Peyer's patches in the intestine and the isolated follicles of the gut-associated lymphoid tissue.[24] The polymeric matrix of PLGA protects the active drug from the hostile environment of the GI lumen. The small size and inimitable surface chemistry of PLGA nanocarriers result in improved adhesion, absorption, and drug transport across the gastrointestinal barrier. After absorption, PLGA slowly degrades into lactic acid and glycolic acid, providing sustained release of the incorporated active agent.

Spherically shaped Dox-NPs were successfully prepared by double emulsion followed by the solvent evaporation method reported previously in the literature.[21] The effect of critical process variables on the characteristics of Dox-NPs was studied and optimized (complete data are not shown) to get the maximum entrapment and desired size of Dox-NPs. But we got the higher (55.4 ± 2.30%) entrapment efficiency using 2% PVA in contrast to 49.00 ± 2.00% as reported by Kalaria et al. using 3% PVA.[21]

The Dox-NPs formulation was freeze-dried by the stepwise freeze-drying process[29,35] using the 5% trehalose as the

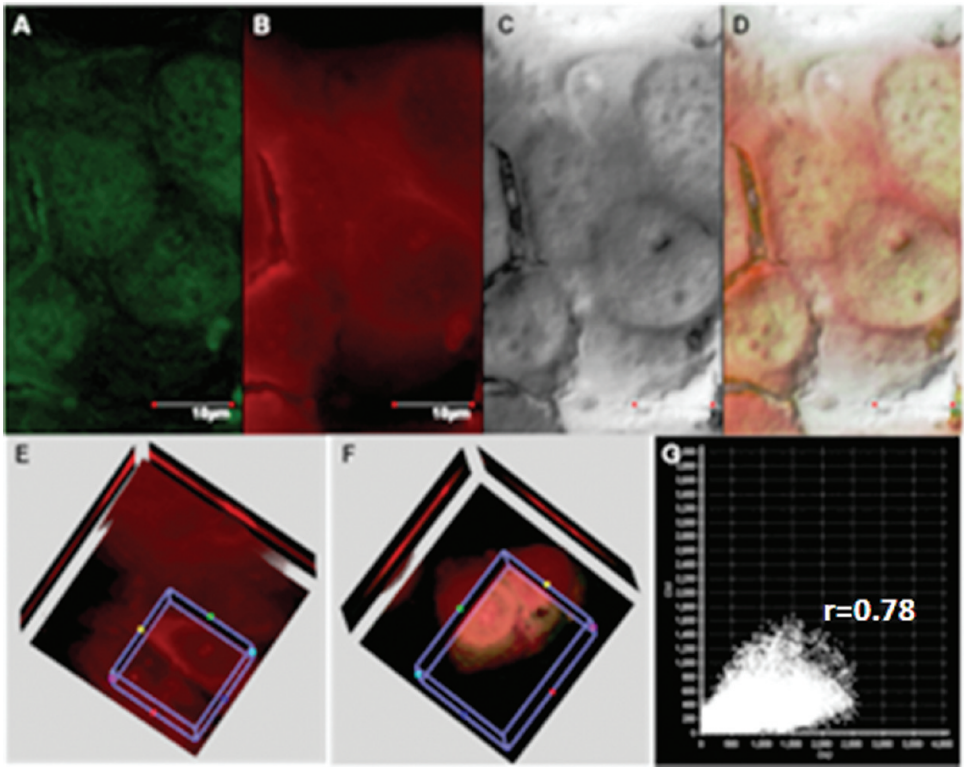

Figure 2. Cellular uptake and nuclear localization of Dox NPs. The figure shows nucleus (A), Dox-NPs (B), and differential interference contrast image (C) of cells. D is the overlay of A, B, and C. E and F are 3D reconstructions of a cell showing Dox NPs (red fluorescence in E) and overlay of Dox NP and AO fluorescence (F). G is a pixel-wise analysis of colocalization of Dox and AO fluorescence.

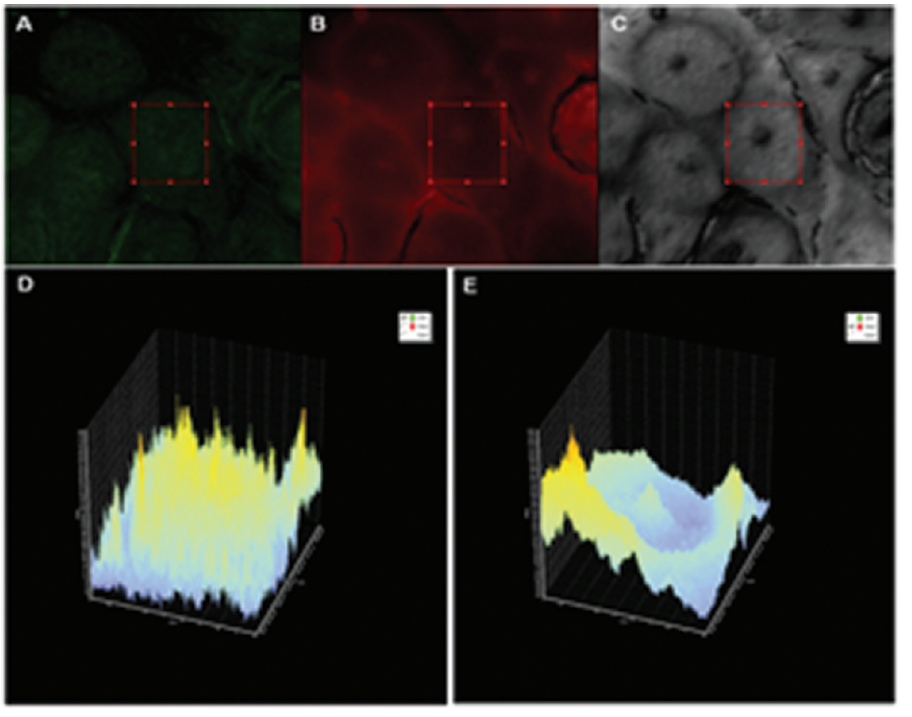

Figure 3. Box analysis of nuclear localization. A, B, and C show nucleus, Dox, and differential interference contrast images, respectively. The box analysis of AO (D) and Dox (E) shows colocalization of Dox fluorescence with nuclear (AO) fluorescence.

cryoprotectant. No significant changes were perceived in the particle size and PDI of nanoparticles following the freeze-drying process. This implied that the 5% trehalose added as the cryoprotectant was sufficient to provide the protection to NPs against

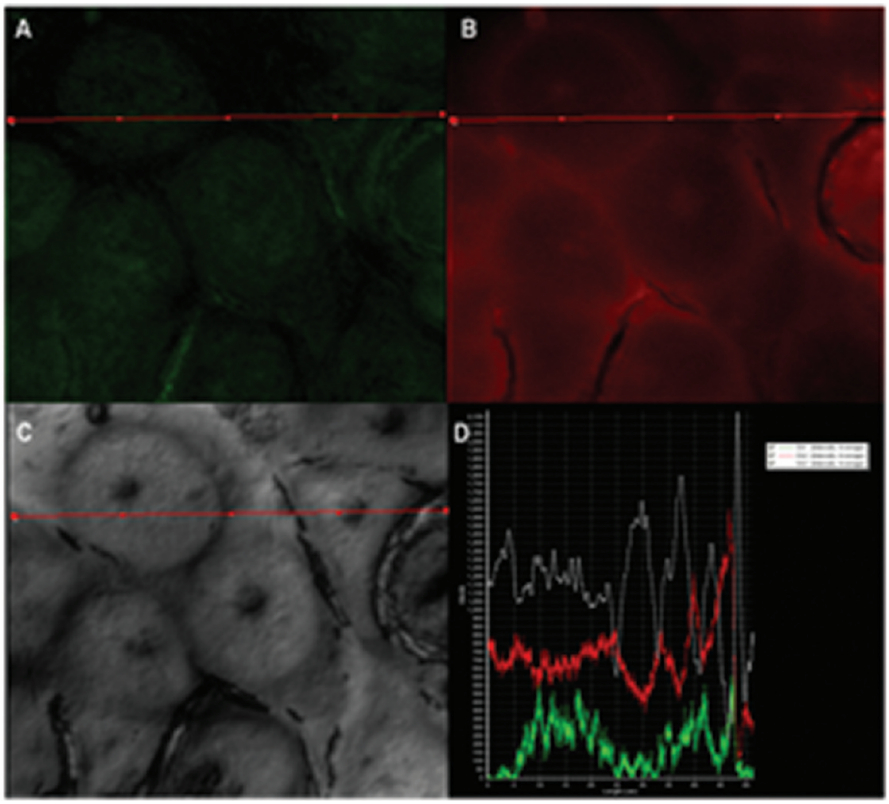

Figure 4. Line analysis of nuclear localization. A, B, and C show nucleus, Dox, and differential interference contrast images, respectively. D shows line analysis of AO (green line) and Dox (red line) fluorescence. The AO and Dox fluorescence show colocalization throughout the line length.

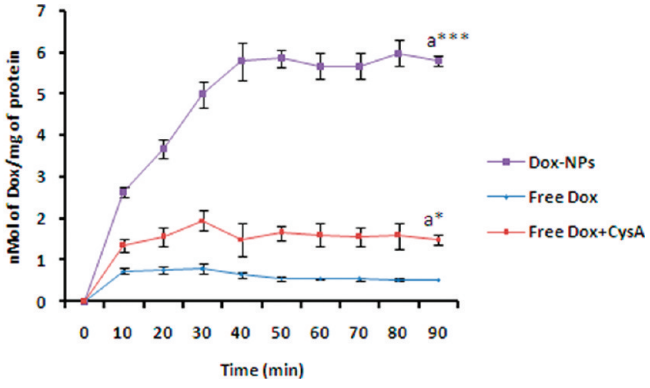

Figure 5. Effect of time of incubation on the Caco-2 cell uptake of Dox and Dox-NPs. Each data point is represented as mean ± SEM (n = 3); (***p < 0.001, *p < 0.05; a vs free Dox all the time points).

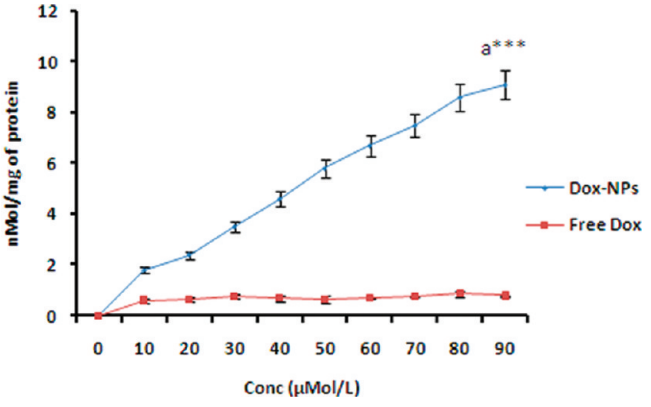

Figure 6. Effect of Dox concentration on the Caco-2 cell uptake of Dox and Dox-NPs. Each data point is represented as mean ± SEM (n = 3); (***p < 0.001; a vs free Dox all the time points).

aggregation. It has been reported that cryoprotectants added during the freeze-drying process prevent aggregation during the freezing and primary drying stage of freeze-drying cycle.[36] When Dox-NPs were freeze-dried without any cryoprotectant, a significant increase (p < 0.05) in the particle size and PDI of NPs was observed, and NPs were not completely redispersed even after shear vortexing. This suggested that the process of freeze-drying in the absence of any cryoprotectant was not sufficient to stabilize the Dox-NPs. The aggregation behavior of the NPs after the freeze-drying was also confirmed by the ratio of particle size after and before freeze-drying and was very close to unity, suggesting that the NPs freeze-dried in presence of trehalose was stable after freeze-drying. No significant (p > 0.05) change was observed in the entrapment efficiency of NPs after the freeze-drying process, and the latter easily dispersed after reconstitution due to the formation of flaccid cake.

Free Dox and Dox-NPs were further evaluated for their in vitro cellular viability on the C127I cell lines by the MTT assay. As evident from Table 3, an insignificant difference (p > 0.05) was noted in the IC_{50} values of free Dox and Dox-NPs treated C127I cells, following 24 h of incubation. This implies that during the initial time course of incubation both free Dox and Dox-NPs are equipotent. However, following 72 h of incubation

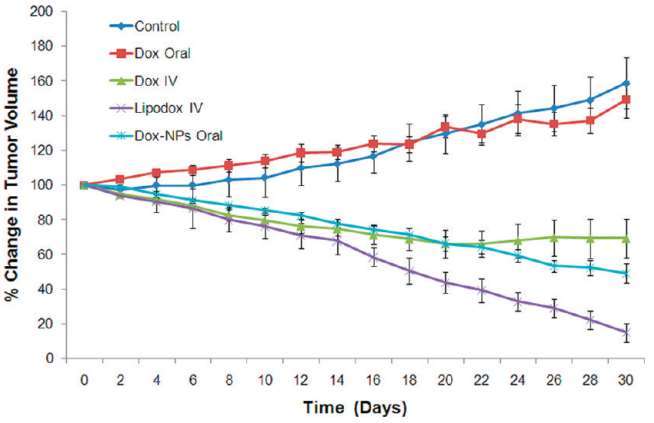

Figure 7. Tumor progressions after oral and intravenous administration of free Dox and oral administration of Dox-NPs (5 mg/kg). Tumor volume was taken as 100% at the start of drug treatment and tumor progression monitored until the end of the study; each data point is represented as the mean ± SEM (n = 6).

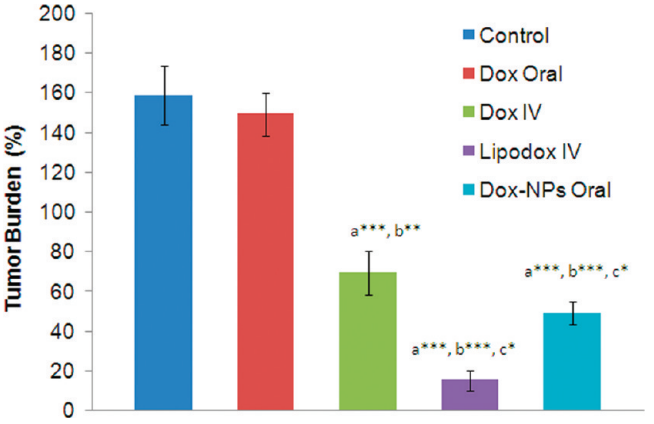

Figure 8. Comparative tumor burdens of Dox-NPs and free Dox solution after 30 days, in DMBA breast cancer animals. Tumor volume was taken as 100% at the start of drug treatment and tumor progression monitored until the end of the study; (***p < 0.001, **p < 0.01, *p < 0.05; (a) vs control, (b) vs Dox oral, and (c) vs Dox IV). Each data point is represented as the mean ± SEM (n = 6).

Dox-NPs were found to be more effective than the free Dox. The observation may be well-explained from the intracellular trafficking behavior of Dox-NPs. As evident from the results of confocal microscopy, following their intracellular uptake, Dox-NPs are rapidly translocated to their site of action, that is, the nucleus.[14] This selective localization augmented sustained release of the drug from the carrier in the vicinity of nucleus, which may be the most plausible reason for higher cytotoxicity of Dox-NPs after 72 h. Further, in the recovery experiments, Dox-NPs showed higher effectiveness as compared to the free drug. While the free drug rapidly washed away, Dox-NPs still retained their activity due to their retention in the cellular milieu, especially in the nuclear region.

It is clear from in vitro cellular uptake studies [Figure 2A−D] that C127I cells incubated with Dox-NPs revealed significant internalization after 3 h. Janes et al. have shown the cellular localization of Dox loaded Chitosan nanoparticles in A375 cells after 24 of incubation.[37] Betancourt and co-workers have also

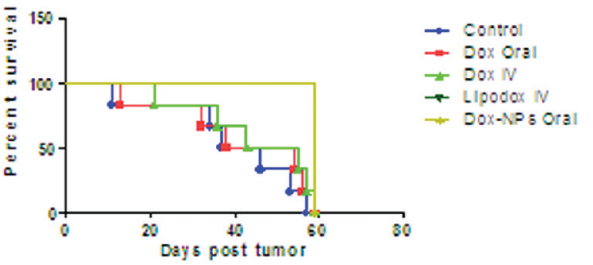

Figure 9. Kaplan−Meier survival curve of tumor bearing rat treated with free Dox, Lipodox, and Dox-NPs at a dose of 5 mg/kg equivalent to Dox. Each data point is represented as the mean ± SEM (n = 6).

shown the increased cellular localization of Dox loaded PLGA nanoparticles in MDA-MB-231 breast cancer cells.[38] To examine the nuclear colocalization of Dox-NPs, C127I cells were stained with a nuclear dye, that is, AO, after washing. As evident from the Figure 2E,F, marked nuclear localization of Dox-NPs was observed. The colocalization determined in the entire field of view (scatter plot) cannot effectively differentiate between fluorescence associated with NPs adhered to the cell surface or from NPs present intracellularly. To confirm the colocalization, line plot analysis was performed which measures variations in fluorescence intensity along a line. However, the line plot determined variations in fluorescence intensity in one dimension. To further confirm the quantitative colocalization results, box-plot analyses were performed which measures the changes in fluorescence intensity in two dimensions, that is, X and Y. Recently, we have also shown the selective nuclear localization tamoxifen loaded PLGA NPs stabilized by PVA.[29] Wong et al. have shown the increased nuclear localization by the encapsulation of Dox in the polymer lipid hybrid nanoparticles.[39] Since the Dox mainly acts on the nuclear region to reveal its therapeutic effects, it is advantageous to have selective localization of Dox-NPs mainly in the nuclear region.[29]

The free Dox suffers from limited oral bioavailability due to its extensive first pass extraction and poor permeability through the GIT. The overexpression of multidrug efflux pump transporter P-glycoprotein (P-gp) in the intestine[40−42] is the main cause of poor permeability of Dox. The caco-2 cell monolayers model is a very well reported tool that mimics intestinal absorptive epithelium and is helpful for studying uptake and transport of drug or nanoparticles across the transepithelial barrier.[51,52] The model is also helpful in evaluating the underlying mechanism of NPs absorption, evaluation of presystemic metabolism, and cytotoxicological assessment. We have evaluated the higher uptake (p < 0.05) of free Dox in presence of a P-gp inhibitor (Cys A), as compared to that treated with free Dox in Caco-2 cell culture model. This could be due to the inhibition of the P-gp efflux pump in the presence of Cys A, a known inhibitor of P-gp. We have not evaluated the Dox uptake from Dox-NPs in presence of Cys A, because it is very well reported that NPs have the special capability of bypassing the P-gp efflux system[27,28] thus overcoming the multidrug resistance which is responsible for the poor oral bioavailability of Dox. Our results are in line with the work carried out by Weilun and co-workers[33] who conducted similar type of experiments with the PAMAM dendrimers loaded with Dox and demonstrated the enhanced oral bioavailability of Dox after the oral administration of PAMAM-Dox complex. When NPs are administered by oral route, they are preferentially absorbed through specialized M-cells of the Peyer's patches in the small

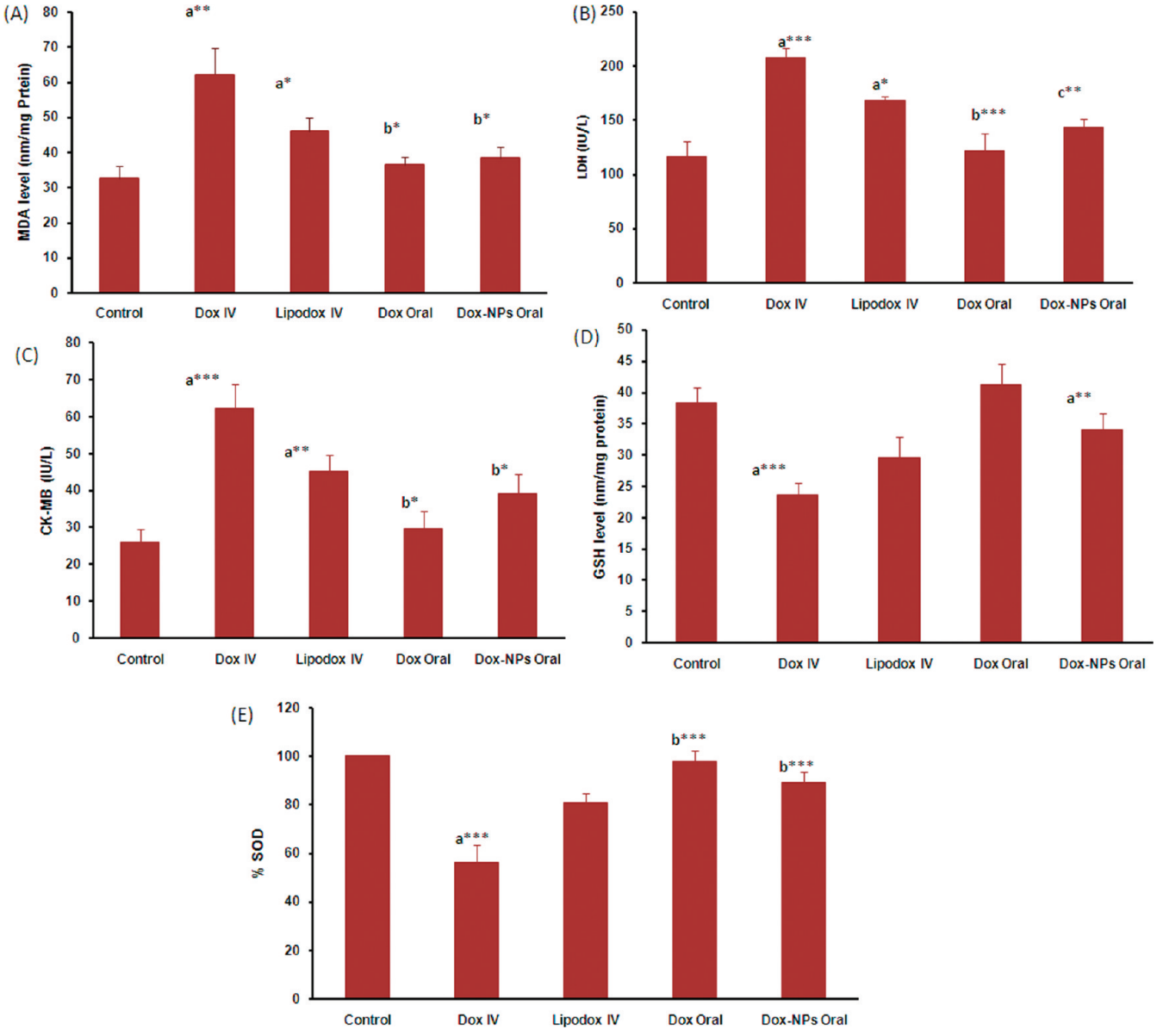

Figure 10. (A) Lipid peroxidation products (MDA) in heart homogenate after one month of the treatment using Dox formulations. (B) LDH levels in plasma after one month of the treatment using Dox formulations. (C) CK-MB levels in plasma after one month of the treatment using Dox formulations. (D) GSH levels in heart homogenate after one month of the treatment using Dox formulations. (E) % SOD levels in heart homogenate after one month of the treatment using Dox formulations. (***$p < 0.001$, **$p < 0.01$, *$p < 0.05$; (a) vs control, (b) vs Dox IV, (c) vs Lipodox IV.)

intestine.[24] Kalaria and his co-workers have reported that PLGA NPs enhanced the oral bioavailability of Dox by 363%, following oral administration. Hence, overall enhancement in the oral bioavailability of Dox via the PLGA nanoparticulate system could be due to the preferential absorption via the M-cells and also bypassing the P-gp efflux system. Further, we have evaluated the antitumor efficacy of Dox-NPs after the oral administration. The antitumor efficacy of different formulation was determined in a DMBA induced breast tumor model.[43−45] Because of the negligible oral bioavailability of Dox, tumor growth was continuously increased comparable to the DMBA control group of animals which received the PBS 7.4. During the initial course of treatment, free Dox administered by the IV route significantly inhibited the tumor growth as compared to the control group. However, in the later course of treatment, the reduction became static due to inefficient accumulation of Dox in the tumor tissues. The insufficient accumulation of Dox in the tumor tissue could be attributed to the overexpression of the P-gp efflux system.[46] As obvious, intravenous administration of marketed formulation of Dox, that is, Lipodox (PEGylated liposomal injection), significantly reduced the tumor growth and tumor burden with highest effectiveness as compared to free Dox (i.v.) and orally administered Dox-NPs. The enhanced efficacy of Lipodox may be attributed to PEGylation, which prolongs the blood circulation time of the liposomal formulation, making it more efficient than the intravenously administered free Dox. The hydrophilic PEG chain enables the liposomal formulation to effectively bypass the reticulo endothelial system (RES) system (adsorption, opsonization, and clearance) and rapidly distribute to the tumor site via enhanced permeation and retention effect (EPR). On the other

hand, orally administered Dox NPs has to cross through numerous barriers of the peroral route so that tumor growth inhibition was almost comparable to that of the intravenously administered Dox and Lipodox in the initial period of the study. However, as previously mentioned, orally administered Dox-NPs can evade the P-gp efflux system of the intestine and subsequently enhanced the oral bioavailability of Dox, which in turn augmented the antitumor efficacy in the later course of treatment. Moreover, the encapsulated Dox releases from the PLGA nanoparticles for a protracted time period and aids in maintaining high local concentration of Dox in the vicinity of tumor tissue. High tumor-specific localization of Dox could be also attributed to the EPR of Dox-NPs.[47] The enhanced survival time of tumor bearing rats following oral administration of Dox-NPs as compared to free Dox administered by oral and IV route was also evident from the Kaplan−Meier survival curve (Figure 9). This could be attributed to the selective accumulation of Dox-NPs in the tumor tissue and upsurge of the drug concentration in tumor tissue as compared to free Dox. The marketed Lipodox formulation also maintained the survival of the tumor bearing animals throughout the study.

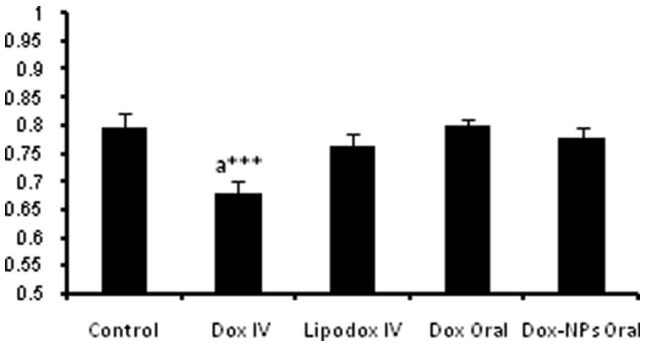

Figure 11. Heart weight of female SD rata after treatment with different Dox formulations on day 30 post-treatment (***$p < 0.001$, (a) vs control).

One of the major adverse effects of Dox is its capability of aggravating the cardiotoxicity after the intravenous injection.[48] The cardiotoxicity of Dox is mainly due to the oxidative stress and subsequent generation of the free radical in the heart muscles.[49] It has been reported that Dox causes oxidative injury to DNA and generates lipid peroxidation.[50] A detailed investigation of cardiotoxicity induced by the free Dox administered intravenously, free Dox, and Dox-NPs administered orally have been carried out by estimating the cardiotoxicity marker levels. Our findings clearly revealed that increase in MDA level in the heart and CK-MB and LDH levels in plasma was observed in the case of cardiotoxicity of Dox. At the same time GSH and SOD levels in the heart homogenate were found to decrease in the case of toxicity. Importantly, marketed formulation reduced the toxicity of free Dox due to its encapsulation in the liposomal formulation, that is, Lipodox. It was clearly observed from Figure 10 that Dox-NPs showed significant reduction in cardiotoxicity that was associated with free drug solution given intravenously. The cardiotoxicity of intravenously administered Dox could be directly correlated with the heart weight. The significant reduction in heart weight in the animal groups treated with intravenous Dox could be attributed to their cardiotoxicity. The heart weight of the animal group treated with intravenously administered Lipodox was not significantly reduced. On the contrary, orally administered Dox-NPs showed marked reduction in toxicity that was reconfirmed by the insignificant change in the heart weight as compared to the control group of animals. We have also carried out histopathological examination of heart tissues. While the normal histopathological structures are preserved in the animal group treated with the Dox-NPs orally, free Dox administered intravenously showed a marked structural damage to cardiac muscles cells due to the generation of cardiotoxicity (Figure 12).

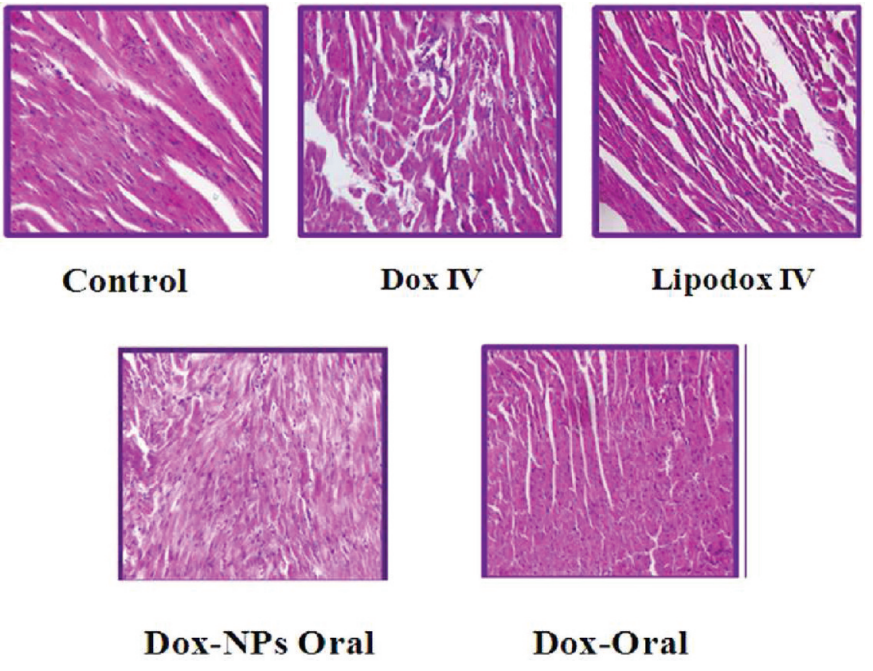

Figure 12. Histological examination of heart after one month treatment of free Dox and Dox-NPs.

5. CONCLUSION

A double emulsion method was employed for the entrapment of Dox in PLGA nanoparticles with the higher entrapment (55.40 ± 2.30%) as compared to the previous reports. To increase the shelf life of prepared nanoparticles, a stepwise freeze-drying method was employed, using 5% trehalose as the cryoprotectant. The encapsulation of Dox in PLGA nanoparticles resulted in enhanced uptake of Dox and accumulation for a protracted period, as compared to the free Dox. Dox-NPs also presented a significant intracellular localization in the nuclear milieu. Dox-NPs also showed concentration and time-dependent higher uptake as compared to the free Dox solution. Taking the consideration of a previous report of oral bioavailability enhancement (363%) by the PLGA NPs, orally administered Dox-NPs have shown a greater antitumor efficacy when evaluated in DMBA induced breast cancer model due to the combined effect of enhanced oral bioavailability and EPR effect. Oral administration of Dox encapsulated in PLGA nanoparticles significantly reduced the Dox induced cardiotoxicity. Although the cardiotoxicity imposed by the orally administered Dox-NPs does not differ significantly than the intravenously administered marketed formulation Lipodox, the oral administration of Dox-NPs could be more effective concerning the patient compliance. The coadministration of Dox-NPs with some antioxidants like Co-Q10 or quercetin to increase the efficacy and ultimately reducing the toxicity of free Dox could be a future implication of successful chemotherapy of Dox. Such studies are currently under progress in our laboratory and will be reported in due course.

AUTHOR INFORMATION

Corresponding Author

*Centre for Pharmaceutical Nanotechnology, Department of Pharmaceutics, National Institute of Pharmaceutical Education and Research (NIPER), Sector 67, SAS Nagar (Mohali), Punjab 160062, India. Telephone: 0172-2292055. Fax: 0172-2214692. E-mail: sanyogjain@niper.ac.in, sanyogjain@rediffmail.com.

Present Addresses

[†]Department of Bioscience, Central University of Punjab, Bathinda, Punjab-151001, India.

ACKNOWLEDGMENT

Authors are thankful to the Director, NIPER, for providing necessary infrastructure facilities and Department of Science & Technology (DST), Government of India, New Delhi, India, for financial support. The histopathological examination carried out at Dr. Vijay Malhotra's Lab, Chandigarh, is also duly acknowledged.

REFERENCES

(1) Travis, L. B.; Curtis, R. E.; Boice, J. D., Jr.; Hankey, B. F.; Fraumeni, J. F., Jr. Second cancers following non-Hodgkin's lymphoma. *Cancer* **1991**, *67* (7), 2002–2009.

(2) Pigram, W. J.; Fuller, W.; Hamilton, L. D. Stereochemistry of intercalation: interaction of daunomycin with DNA. *Nat. New Biol.* **1972**, *235* (53), 17–9.

(3) Ogden, A. Method of treating multiple sclerosis. U.S. Patent 10438131, 2003.

(4) Perez, A. T.; Domenech, G. H.; Frankel, C.; Vogel, C. L. Pegylated Liposomal Doxorubicin (Doxil) for Metastatic Breast Cancer: The Cancer Research Network, Inc., Experience. *Cancer Invest.* **2002**, *20* (s2), 22–29.

(5) Gabizon, A.; Shmeeda, H.; Barenholz, Y. Pharmacokinetics of pegylated liposomal Doxorubicin: review of animal and human studies. *Clin. Pharmacokinet.* **2003**, *42* (5), 419–436.

(6) De Beer, E. L.; Bottone, A. E.; Voest, E. E. Doxorubicin and mechanical performance of cardiac trabeculae after acute and chronic treatment: a review. *Eur. J. Pharmacol.* **2001**, *415* (1), 1–11.

(7) Sangeetha, P.; Das, U. N.; Koratkar, R.; Suryaprabha, P. Increase in free radical generation and lipid peroxidation following chemotherapy in patients with cancer. *Free Radical Biol. Med.* **1990**, *8* (1), 15–19.

(8) Olson, R. D.; Mushlin, P. S. Doxorubicin cardiotoxicity: analysis of prevailing hypotheses. *FASEB J.* **1990**, *4* (13), 3076–86.

(9) Singal, P. K.; Iliskovic, N. Doxorubicin-induced cardiomyopathy. *N. Engl. J. Med.* **1998**, *339* (13), 900–905.

(10) Olson, R. D.; Mushlin, P. S.; Brenner, D. E.; Fleischer, S.; Cusack, B. J.; Chang, B. K.; Boucek, R. J. Doxorubicin cardiotoxicity may be caused by its metabolite, doxorubicinol. *Proc. Natl. Acad. Sci. U.S.A.* **1988**, *85* (10), 3585–9.

(11) Tang, X. H.; Xie, P.; Ding, Y.; Chu, L. Y.; Hou, J. P.; Yang, J. L.; Song, X.; Xie, Y. M. Synthesis, characterization, and in vitro and in vivo evaluation of a novel pectin-adriamycin conjugate. *Bioorg. Med. Chem.* **2010**, *18* (4), 1599–609.

(12) Yeung, T. K.; Hopewell, J. W.; Simmonds, R. H.; Seymour, L. W.; Duncan, R.; Bellini, O.; Grandi, M.; Spreafico, F.; Strohalm, J.; Ulbrich, K. Reduced cardiotoxicity of doxorubicin given in the form of N-(2-hydroxypropyl) methacrylamide conjugates: an experimental study in the rat. *Cancer Chemother. Pharmacol.* **1991**, *29* (2), 105–111.

(13) Reddy, L. H.; Murthy, R. S. Pharmacokinetics and biodistribution studies of Doxorubicin loaded poly (butyl cyanoacrylate) nanoparticles synthesized by two different techniques. *Biomed. Pap. Med. Fac. Palacky Univ. Olomouc* **2004**, *148* (2), 161–6.

(14) Upadhyay, K. K.; Bhatt, A. N.; Mishra, A. K.; Dwarakanath, B. S.; Jain, S.; Schatz, C.; Le Meins, J. F.; Farooque, A.; Chandraiah, G.; Jain, A. K.; Misra, A.; Lecommandoux, S. The intracellular drug delivery and anti tumor activity of doxorubicin loaded poly(γ-benzyl l-glutamate)-b-hyaluronan polymersomes. *Biomaterials* **2010**, *31* (10), 2882–92.

(15) Kattan, J.; Droz, J. P.; Couvreur, P.; Marino, J. P.; Boutan-Laroze, A.; Rougier, P.; Brault, P.; Vranckx, H.; Grognet, J. M.; Morge, X. Phase I clinical trial and pharmacokinetic evaluation of doxorubicin carried by polyisohexylcyanoacrylate nanoparticles. *Invest. New Drugs* **1992**, *10* (3), 191–199.

(16) Bisht, S.; Maitra, A. Dextran-doxorubicin/chitosan nanoparticles for solid tumor therapy. *Wiley Interdiscip. Rev. Nanomed. Nanobiotechnol.* **2009**, *1* (4), 415–425.

(17) Mitra, S.; Gaur, U.; Ghosh, P. C.; Maitra, A. N. Tumour targeted delivery of encapsulated dextran-doxorubicin conjugate using chitosan nanoparticles as carrier. *J. Controlled Release* **2001**, *74* (1−3), 317–323.

(18) Yadav, A. K.; Mishra, P.; Mishra, A. K.; Jain, S.; Agrawal, G. P. Development and characterization of hyaluronic acid-anchored PLGA nanoparticulate carriers of doxorubicin. *Nanomedicine* **2007**, *3* (4), 246–257.

(19) Yadav, A. K.; Mishra, P.; Jain, S.; Mishra, A. K.; Agrawal, G. P. Preparation and characterization of HA-PEG-PCL intelligent core-corona nanoparticles for delivery of doxorubicin. *J. Drug Target.* **2008**, *16* (6), 464–478.

(20) Varma, M. V. S.; Khandavilli, S.; Ashokraj, Y.; Jain, A.; Dhanikula, A.; Sood, A.; Thomas, N. S.; Pillai, O.; Sharma, P.; Gandhi, R. Biopharmaceutic classification system: a scientific framework for pharmacokinetic optimization in drug research. *Curr. Drug Metab.* **2004**, *5* (5), 375–388.

(21) Kalaria, D. R.; Sharma, G.; Beniwal, V.; Ravi Kumar, M. N. V. Design of biodegradable nanoparticles for oral delivery of doxorubicin: in vivo pharmacokinetics and toxicity studies in rats. *Pharm. Res.* **2009**, *26* (3), 492–501.

(22) Astete, C. E.; Sabliov, C. M. Synthesis and characterization of PLGA nanoparticles. *J. Biomater. Sci., Polym. Ed.* **2006**, *17* (3), 247–289.

(23) Govender, T.; Stolnik, S.; Garnett, M. C.; Illum, L.; Davis, S. S. PLGA nanoparticles prepared by nanoprecipitation: drug loading and release studies of a water soluble drug. *J. Controlled Release* **1999**, *57* (2), 171–185.

(24) Florence, A. T. The oral absorption of micro-and nanoparticulates: neither exceptional nor unusual. *Pharm. Res.* **1997**, *14* (3), 259–266.

(25) Clark, M.; Jepson, M. A.; Hirst, B. H. Exploiting M cells for drug and vaccine delivery. *Adv. Drug Delivery Rev.* **2001**, *50* (1−2), 81–106.

(26) Hussain, N.; Jaitley, V.; Florence, A. T. Recent advances in the understanding of uptake of microparticulates across the gastrointestinal lymphatics. *Adv. Drug Delivery Rev.* **2001**, *50* (1−2), 107–142.

(27) Dong, X.; Mattingly, C. A.; Tseng, M. T.; Cho, M. J.; Liu, Y.; Adams, V. R.; Mumper, R. J. Doxorubicin and paclitaxel-loaded lipid-based nanoparticles overcome multidrug resistance by inhibiting P-glycoprotein and depleting ATP. *Cancer Res.* **2009**, *69* (9), 3918–26.

(28) Bardelmeijer, H. A.; Beijnen, J. H.; Brouwer, K. R.; Rosing, H.; Nooijen, W. J.; Schellens, J. H. M.; van Tellingen, O. Increased oral bioavailability of paclitaxel by GF120918 in mice through selective modulation of P-glycoprotein. *Clin. Cancer Res.* **2000**, *6* (11), 4416–21.

(29) Jain, A. K.; Swranakar, N. K.; Chandraiah, G.; Preet, S. R.; Jain, S. The effect of the oral administration of polymeric nanoparticles on the efficacy and toxicity of tamoxifen. *Biomaterials* **2011**, *32* (2), 503–15.

(30) Kogure, K.; Hama, S.; Manabe, S.; Tokumura, A.; Fukuzawa, K. High cytotoxicity of α-tocopheryl hemisuccinate to cancer cells is due to failure of their antioxidative defense systems. *Cancer Lett.* **2002**, *186* (2), 151–156.

(31) Yin Win, K.; Feng, S. S. Effects of particle size and surface coating on cellular uptake of polymeric nanoparticles for oral delivery of anticancer drugs. *Biomaterials* **2005**, *26* (15), 2713–2722.

(32) Dong, Y.; Feng, S. S. Poly (D,L-lactide-co-glycolide)/montmorillonite nanoparticles for oral delivery of anticancer drugs. *Biomaterials* **2005**, *26* (30), 6068–6076.

(33) Ke, W.; Zhao, Y.; Huang, R.; Jiang, C.; Pei, Y. Enhanced oral bioavailability of doxorubicin in a dendrimer drug delivery system. *J. Pharm. Sci.* **2008**, *97* (6), 2208–2216.

(34) Bradford, M. M. A rapid and sensitive method for the quantitation of microgram quantities of protein utilizing the principle of protein-dye binding. *Anal. Biochem.* **1976**, *72* (1−2), 248–254.

(35) Jain, S.; Mittal, A.; Jain, K.; Mahajan, R.; Singh, D. Cyclosporin A Loaded PLGA nanoparticle: preparation, optimization, in-vitro characterization and stability studies. *Curr. Nanosci.* **2010**, *6* (4), 422–431.

(36) Abdelwahed, W.; Degobert, G.; Stainmesse, S.; Fessi, H. Freeze-drying of nanoparticles: Formulation, process and storage considerations. *Adv. Drug Delivery Rev.* **2006**, *58* (15), 1688–1713.

(37) Janes, K. A.; Fresneau, M. P.; Marazuela, A.; Fabra, A.; Alonso, M. J. Chitosan nanoparticles as delivery systems for doxorubicin. *J. Controlled Release* **2001**, *73* (2−3), 255–267.

(38) Betancourt, T.; Brown, B.; Brannon-Peppas, L. Doxorubicin-loaded PLGA nanoparticles by nanoprecipitation: preparation, characterization and in vitro evaluation. *Nanomedicine* **2007**, *2* (2), 219–232.

(39) Wong, H. L.; Bendayan, R.; Rauth, A. M.; Xue, H. Y.; Babakhanian, K.; Wu, X. Y. A mechanistic study of enhanced doxorubicin uptake and retention in multidrug resistant breast cancer cells using a polymer-lipid hybrid nanoparticle system. *J. Pharmacol. Exp. Ther.* **2006**, *317* (3), 1372–81.

(40) Bellamy, W. T. P-glycoproteins and multidrug resistance. *Annu. Rev. Pharmacol. Toxicol.* **1996**, *36* (1), 161–183.

(41) Fojo, A. T.; Ueda, K.; Slamon, D. J.; Poplack, D. G.; Gottesman, M. M.; Pastan, I. Expression of a multidrug-resistance gene in human tumors and tissues. *Proc. Natl. Acad. Sci. U.S.A.* **1987**, *84* (1), 265–9.

(42) Borst, P.; Schinkel, A. H.; Smit, J. J. M.; Wagenaar, E.; Van Deemter, L.; Smith, A. J.; Eijdems, E.; Baas, F.; Zaman, G. J. R. Classical and novel forms of multidrug resistance and the physiological functions of P-glycoproteins in mammals. *Pharmacol. Ther.* **1993**, *60* (2), 289–299.

(43) Kaufmann, Y.; Kornbluth, J.; Feng, Z.; Fahr, M.; Schaefer, R. F.; Klimberg, V. S. Effect of glutamine on the initiation and promotion phases of DMBA-induced mammary tumor development. *J. Parenter. Enteral Nutr.* **2003**, *27* (6), 411–8.

(44) Rehm, S. Chemically induced mammary gland adenomyoepitheliomas and myoepithelial carcinomas of mice. Immunohistochemical and ultrastructural features. *Am. J. Pathol.* **1990**, *136* (3), 575–84.

(45) Bhardwaj, V.; Ankola, D. D.; Gupta, S. C.; Schneider, M.; Lehr, C. M.; Kumar, M. PLGA nanoparticles stabilized with cationic surfactant: safety studies and application in oral delivery of paclitaxel to treat chemical-induced breast cancer in rat. *Pharm. Res.* **2009**, *26* (11), 2495–2503.

(46) Ballinger, J. R.; Bannerman, J.; Boxen, I.; Firby, P.; Hartman, N. G.; Moore, M. J. Technetium-99m-tetrofosmin as a substrate for P-glycoprotein: in vitro studies in multidrug-resistant breast tumor cells. *J. Nucl. Med.* **1996**, *37* (9), 1578–82.

(47) Maeda, H. The tumor blood vessel as an ideal target for macromolecular anticancer agents. *J. Controlled Release* **1992**, *19* (1−3), 315–324.

(48) Turakhia, S.; Venkatakrishnan, C. D.; Dunsmore, K.; Wong, H.; Kuppusamy, P.; Zweier, J. L.; Ilangovan, G. Doxorubicin-induced cardiotoxicity: direct correlation of cardiac fibroblast and H9c2 cell survival and aconitase activity with heat shock protein 27. *Am. J. Physiol. Heart Circ. Physiol.* **2007**, *293* (5), H3111–21.

(49) Quiles, J. L.; Huertas, J. R.; Battino, M.; Mataix, J.; Ramírez-Tortosa, M. C. Antioxidant nutrients and adriamycin toxicity. *Toxicology* **2002**, *180* (1), 79–95.

(50) Mataix, J.; Manas, M.; Quiles, J.; Battino, M.; Cassinello, M.; Lopez-Frias, M.; Huertas, J. R. Coenzyme Q content depends upon oxidative stress and dietary fat unsaturation. *Mol. Aspects Med.* **1997**, *18*, 129–135.

(51) Hilgers, A. R.; Conradi, R. A.; Burton, P. S. Caco-2 cell monolayers as a model for drug transport across the intestinal mucosa. *Pharm. Res.* **1990**, *7*, 902–910.

(52) Artursson, P. Epithelial transport of drugs in cell culture. I: A model for studying the passive diffusion of drugs over intestinal absorbtive (Caco 2) cells. *J. Pharm. Sci.* **1990**, *79* (6), 476–482.